Novel ultrasonic technology for the digitalization and wireless transformation of portable three-ball incentive spirometers

Jih-Shuin Jerng[1], Szu-An Chen[2], Chien-Hung Liao[2], Kang-Yun Lee[3], Su-Yen Hao[4,5,6,7], Chin-Hung Wei[8,9], Hsu-Tung Lee[10,11], Johnson Lin[12], Min-Huan Wu[13], Tai-Horng Young[14], Cheng-Yu Tsai[3], Chien-An Liao[2,14*], and Wen-Te Liu[3*]

[1]Division of Pulmonary Medicine, Department of Internal Medicine, National Taiwan University Hospital, Taipei, Taiwan

[2]Department of Trauma and Emergency Surgery, Chang Gung Memorial Hospital, Taoyuan, Taiwan

[3]Division of Pulmonary Medicine, Department of Internal Medicine, Shuang Ho Hospital, Taipei Medical University, New Taipei City, Taiwan

[4]Department of Surgery, School of Medicine, College of Medicine, Taipei Medical University, Taipei, Taiwan

[5]Division of General Surgery, Department of Surgery, Shuang Ho Hospital, Taipei Medical University, New Taipei City, Taiwan

[6]Division of General Surgery, Department of Surgery, School of Medicine, College of Medicine, Taipei Medical University, Taipei, Taiwan

[7]TMU Research Center of Cancer Translational Medicine, Taipei Medical University, Taipei, Taiwan

[8]Division of Pediatric Surgery, Department of Surgery, Shuang Ho Hospital, New Taipei City, Taiwan

[9]Department of Surgery, School of Medicine, College of Medicine, Taipei Medical University, Tai Cancer Prevention and Control Center, Taichung Veterans General Hospital, Taichung, Taiwan

[10]College of Medicine, National Chung Hsing University, Taichung, Taiwan

[11]Graduate Institute of Medical Sciences, National Defense Medical Center, Taipei, Taiwan

[12] Department of Internal Medicine, Mackay Memorial Hospital, Taipei, Taiwan

[13]Senior Life and Innovation Technology Center, Tunghai University, Taichung, Taiwan

[14]Institute of Biomedical Engineering, College of Medicine and College of Engineering, National Taiwan University, Taipei, Taiwan

[*]**Corresponding authors:**

Chien-An Liao, *MD*

Department of Trauma and Emergency Surgery, Chang Gung Memorial Hospital, Taoyuan, Taiwan

Email:

Wen-Te Liu, *MD, PhD*

Associate Professor, School of Respiratory Therapy, College of Medicine, Taipei Medical University Address: No. 250, Wuxing Street, Taipei 110301, Taiwan

Telephone: +886-

Fax: +886-

E-mail:

All authors have read and approved the final version of the manuscript.

Abstract

Background: Portable devices such as three-ball incentive spirometers (TBISs) remain an essential means in current health-care practice of monitoring patients' physiological function. However, achieving digitalization and wireless transformation of these devices without altering their original design and functionality is challenging.

Methods: We propose a novel design in which infrared (IR) detection and an ultrasound (US) generating module are integrated with a normal TBIS. The US module generates US signals at 18, 20, and 22 kHz, which correspond to the movements of the three balls of TBISs during deep breathing exercises. We tested various distances and modes of airflow generation and compared US signals recorded using different smartphones with visual observations.

Results: No background noise interference from smartphones within the range of 18–22 kHz was detected at over 90 dB, indicating the ultrasonic wireless module exhibits real-time detection capability and effectively captures signals at a distance of 10–160 cm. The primary indicator is floating on the maximum duration by visional and ultrasonic signals correlation is 0.9993–0.9999 at the three balls status.

Conclusions: This proposed design in which IR detection is coupled with US module signal transmission exhibits promise as a means of digitalization and wireless transformation of conventional nonelectronic portable devices used to monitor physiological function. This approach is cost effective and enables health professionals and patients to review and assess respiratory performance through telemedicine.

Keywords

Incentive spirometer, wireless transformation, ultrasound signals, pulmonary function test

Introduction

Monitoring respiratory function using mobile devices has been increasingly promoted in recent years, partly because the COVID-19 pandemic led to a need for alternatives to in-person medical care. Portable devices, such as oximeters, peak flow meters, respiratory meters, and spirometers, have become widely used, and many of these devices have health-promoting functions.[1,2] Digitalization and wireless connectivity in these monitoring devices are crucial to their being able to be seamlessly integrated with mobile devices, such as smartphones, because these functions not only afford convenience but also facilitate cloud synchronization, which plays a pivotal role in telemedicine. Monitoring devices designed to be electronic devices provide invaluable data that can be used for diagnosing and monitoring health status, tracking disease conditions, and assisting with training and rehabilitation during recovery from disease.[3–5] Therefore, digitalization and wireless transformation of monitoring devices not initially designed to be electronic devices, such as incentive spirometers, is crucial.

An incentive spirometer, also known as a breathing exerciser, is used to train respiratory muscles. This device increases the vital breathing capacity of patients undergoing chest or abdominal surgeries and those with conditions such as bronchial asthma, chronic obstructive pulmonary disease, and pulmonary infection. Incentive spirometers are classified on the basis of whether they measure breathing flow or air volume, their mechanical principles, and whether training targets inspiratory or expiratory strength.[6,7] A typical three-ball incentive spirometer (TBIS) comprises a nonelectronic PVC body with a pipeline and compartments in which three floatable balls are loaded. These balls serve as indicators of inspiratory performance, which is analyzed using a a semiquantitative scale. In addition, a TBIS contains a mouthpiece and a connecting tube, which are used to deliver the airflow. Modified versions of TBISs have been developed to measure expiratory strength by using a

reverse holding and blocking mechanism or have been equipped with oxygen supply connectors. TBISs, typically priced between US$10 and US$30, are durable and inexpensive, and they can be easily cleaned with water. However, limited information is available in the literature regarding the digitalization and wireless transformation of TBISs.

Researchers have applied methods such as using smartphone cameras combined with artificial intelligence analysis and infrared (IR), whistle-sound, or voice signals to determine inspiratory or expiratory function. Although these researchers have made considerable advances, challenges related to the accuracy and cost of the methods persist.[8,9] Regarding smartphone computing and storage, wireless functionality must be prioritized. Bluetooth and WiFi are necessary for the microcontroller units and storage IC to synchronize data and establish connections between smartphones, tablets, and computers and laptops. Smartphones and other electronic devices have basic sensors that can detect audio, light, and magnetic forces. However, their application in wireless protocols is limited due to constraints related to transmission distance and background noise. However, ultrasonic frequency exceeds the 20 kHz audio range and is infrequently affected by interference. Smartphones can record audio at a sampling rate of 44.1 kHz, referred to as Hi-Fi, or 48 kHz, referred to as Hi-Res, through audio codecs. Available file formats for such audio recordings include wav, mp3, and real-time pulse code modulation.

In the current study, we used ultrasonic signals in a wireless protocol for evaluating the performance of incentive spirometers, identified their limitations, and introduced a new method for enhancing traditional plastic medical devices by adding wireless and digital functionalities. Our ultrasonic wireless module can be used to assist patients with COVID-19 with restoring their lung function and improving their quality of life through telehealth.

Method

Proposed design

Our proposed design incorporates three IR sensors mounted on a jumper board assembled with ultrasound modules and an algorithm system. This assembly is attached to the outer surface of the columns of a TBIS (GaleMed, Taipei, Taiwan; Fig. 1a). This TBIS model can be placed on reverse hold, subjected to suction by using an SDI 3-L syringe, and tested using an inspiration breath to confirm the sensitivity of the IR ultrasound system. The ultrasonic modules, which operate from a 5-V DC power supply, generate signals at 18, 20, and 22 kHz. This power supply can be replaced with two coin batteries (CR-2032) that together supply 6V. A sensor tracking the movements of the three balls of TBIS devices, which indicate an inspiratory flow rate of 600 mL/s (pink), 900 mL/s (yellow), and 1,200 mL/s (green), generates ultrasonic signals for the balls at 18, 20, and 22 kHz, respectively. These frequencies were selected on the basis of background ultrasonic noise. With the use of the Spectroid app, no substantial background ultrasound signals were detected at a frequency of >18 kHz. This real-time analysis in addition to Windows Spek spectrogram recordings confirmed that the selected frequencies were suitable for the office environment in which the study was performed.

Detection of ultrasonic signals

We detected the movement of the TBIS balls when the device was in a reverse position and subjected to suction with a 3-L syringe. In addition, we used real-life inspiration breaths to move the TBIS balls. For TBISs, the duration of the period in which each ball floats at the top of its respective column is measured. Count and subsequent analysis can be performed by capturing video and audio recordings, which can later be played at a slow speed for meticulous observation. In the current study, patients were asked to complete several random deep breaths using the TBIS. Adobe Audition and Premiere Pro were used to determine the

duration of the period in which each ball floated at the top of its column at a resolution of 1/10 second.

We used smartphones with the Android operating system (Google Pixel 5) or the iOS operating system (Apple iPhone 13 Pro). These phones contained audio recorder apps that capture sounds in the uncompressed pulse code modulation wave format. Additionally, the phones contained real-time spectrum or spectrogram apps. It can also be presented in the real-time spectrum spectrogram and compared with Arduino UNO to emit the same frequencies signals in the ultrasonic ranges. To enhance audio recording and sampling performance, we integrated an external USB-microphone (MIC) with a Hi-Res audio codec and an MEM microphone. These devices were connected to the smartphones with a type C cable (for the Android phones) or a lightning adapter (for the iOS phones). Audio recorder apps (Amazing MP3 recorders, Version 0.10.78, for the Android phones; Apogee MetaRecorder, Version 2.2.1, for the iOS phones) and real-time spectrogram apps (USB Audio Recorder Pro, Version 1.6.1.0, for the Android phones; Spectroid, for the iOS phones) were used. A real-time spectrogram app (Spectroid, Version 1.1.1) was also used for the Android phones.

After capturing the receiving of the ultrasound signals, we recorded audio intensities from ultrasonic wireless modules at three frequencies (i.e., 18, 20, and 22 kHz). These recordings were saved in the high-quality .wav format. To assess the signal-to-noise ratio, we conducted tests at several distances (10, 20, 40, 80, and 160 cm, Figure 1b) over a duration of 60 s. In addition, we played music through a computer speaker using Hi-Res player software and achieved an intensity of >80 dB from a distance of 50 cm. We analyzed the audio files to determine the signal-to-noise ratio by using the free and open-source spectrogram software Spek (version 0.8.2 for Windows, released on February 24, 2013) licensed under GPLv3, Adobe Audition, and Premiere Pro Creative Cloud (https://www.adobe.com/creativecloud/plans.html). To complete comparisons, we used preset

ultrasonic signals at 23 kHz (Arduino UNO) and 19 kHz (KardiaMobile, AliveCor) and determined the responsiveness of the smartphone microphones to the ultrasonic signals. KardiaMobile is a device designed to receive and analyze heartbeats and echocardiogram (ECG) readings using a smartphone's microphone. This device is mounted on a metal coin with electrodes and circuit path power,[10] and the Kardia app (version 5.25.0) is used to determine the user's ECG readings and export ECG graphs in a PDF format.

Comparison with visual observations

We analyzed the correlation between the recorded ultrasonic signals and visual observations when one of the investigators of this study performed deep breathing using our TBIS (Figure 1c). The investigator completed this action approximately 30 to 50 times to cause one to three balls to float at the top of the columns. Video and audio recordings of the process were obtained. The time in which each ball remained at the top was analyzed using default ultrasound readings, which were compared with visual observations made during slow playback of the recordings.

This study was reviewed and approved by the Institutional Review Board of Chang Gung Memorial Hospital (2204250016). Genius (Genius Holding LLC, Taipei, Taiwan) provided the devices and apps.

Results

Detection of ultrasonic signals generated by the module and comparison of results for different smartphones

The IR plus ultrasonic wireless modules emitted ultrasonic signals at 18, 20, and 22 kHz. Both the Android and the iOS smartphones could receive signals at a distance of 10 to 160 cm (Fig. 2a and 2e and Table 1). However, the 23-kHz ultrasonic signal produced by the

Arduino was recorded only on the Pixel 5 and on the external USB-MIC devices that had been connected to each type of smartphone (Fig. 2f and 2g). The iOS smartphone could not record the 23-kHz ultrasonic signal (Fig. 2b) or any frequencies exceeding 22 kHz produced by the Arduino. This limitation was observed across several apps, even those with a 48-kHz sampling rate for the file formats. When the 22-kHz frequency was analyzed, a slightly weaker response was noted on the iOS device than that on the Android device or on the devices when an external USB-MIC was connected (Fig. 2c).

Audio signals between 15 and 22 kHz were clear and pronounced at a distance of 10 to 160 cm; the 16-kHz audio signal was accompanied by the combined ultrasonic frequencies of 18, 20, and 22 kHz made by the pilot module board (Fig. 2a, 2c–2e, 2g, 2h) and could be filtered by the commercial electronic circuit board. According to clinical experts, a distance of 50–100 cm is optimal for simultaneously using a TBIS and monitoring the results using an app on a smartphone or tablet. Although the Arduino-generated 23-kHz signal was not recorded on the iOS phone (Fig. 2b), it was recorded on the Android phone (Fig. 2f). This finding was corroborated by spectrograms for the iOS phone (Table 1). To enhance the iOS phone's audio sensitivity, a Genius external MIC was connected to the phone by using a lightning-to-USB camera adapter (Fig 2c). This setup enhanced the device's auditory response, enabling it to record the 24-kHz ultrasonic signal emitted by the Arduino. Although the KardiaMobile's 19-kHz signal could be recorded at a distance of 160 cm (Fig 2d), the app exhibited poor signal strength when human fingers executed the standard ECG test procedure, especially when the distance between the smartphone and KardiaMobile was greater than 30 cm. The Android phone recorded clear ultrasonic signals, including those at the frequencies of 18, 20, and 22 kHz that were emitted by the TBIS (Fig. 2e); that at the frequency of 23kHz emitted by Arduino (Fig. 2f); and that at the frequency of 19 kHz emitted by KardiaMobile (Fig. 2h). External microphones can be easily connected to smartphones by

using a type C to type C cable; however, some Android smartphones might require the initiation of the OTG function (Fig. 2c and 2g). In the present study, when the IR ultrasonic wireless module emitted 18, 20, and 22 kHz together, a 16-kHz signal was also emitted. The use of another piezoelectric element can improve the purity of ultrasonic signals. A 16-kHz signal can be heard by human ears and detected using a decibel meter. However, human sensitivity to this frequency varies across individuals. In the present study, we analyzed ultrasonic audio files by using spectrograms to confirm that the ultrasonic signals would not interfere between the ultrasonic wireless incentive spirometer and KardiaMobile.

Discrimination from noise signals

The Spectroid app, which was used for real-time analysis, and Windows Spek, which was used for spectrogram evaluation, did not detect any significant background ultrasounds at >18 kHz. Background noise and sensitivity levels differ with the ultrasonic frequency because of factors such as environmental conditions, audio codecs, and microphone responses. In the present study, the experiments were conducted in a typical office and laboratory facility. In this environment, the background noise was below 40–50 dB, as measured using a dB meter, and no significant ultrasonic noise was detected. Adobe Audition was used to analyze audio files. We used dB below full scale as the unit of intensity, with 0 representing the maximum achievable level.

The recordings and spectrogram analyses for the iOS and Android phones for the standard office environment of this study revealed no significant ultrasounds (Fig. 3a and 3e). In addition, in this environment, the ultrasonic signals were clear (Fig. 3b and 3f), and the Hi-Res music played at an average of 90 dB was recorded by the dB meter (Fig. 3c and 3g). The ultrasonic signals emitted by the IR wireless ultrasonic module were adequately clear and able to indicate the status of the balls within the TBIS columns when the distance between the smartphone microphone and TBIS was 40 cm (Fig. 3d and 3h and Table 2).

The signal plus noise intensity was lower at 22 kHz for the iOS phone. This finding may be attributable to limitations related to the audio codec or defaults in the audio application programming interface. Connecting an external MIC through a USB cable to the iOS or Android phones significantly improved the clarity of the ultrasonic frequencies, even at 24–48 kHz. However, ultrasonic microphones are not easily available and can cost more than US$200. Furthermore, such microphones may not be compatible with all smartphones; in some cases, they may be compatible only with specific apps provided by the microphone manufacturers.

Audio signals generated by the IR plus ultrasonic TBIS were determined in the reverse status (Fig. 4a, 4d), inspired by 3L syringe suction (Fig. 4b, 4e). And human inspiratory to move the balls at the IR sensors' location and trigger the electronic (Fig. 4c, 4f). Ultrasounds have high sensitivity when emitted at 18, 20, or 22 kHz, and these frequencies were detectable on both the Android and the iOS phones. In TBIS devices, human breathing and suction change the pressure experienced by the three balls, leading to the movement of one to three balls, depending on the airflow rate. Because voice signals can overlap at the same frequencies, ultrasonic signals can be used to effectively establish a threshold for determining the on/off status of events. The intensity of these ultrasonic signals can be enhanced when necessary by adjusting the voltage and current to ensure efficient transmission over long distances. In the present study, when the TBIS was used, the balls produced noise without latency across various frequencies when they reached the top of or fell in their respective columns. The IR sensors emitted IR signals and controlled ultrasonic modules. This enabled the modules to emit default frequencies that directly indicated the on/off status of the TBIS, eliminating the need for a microcontroller unit.

In our spectrogram analysis, no overlapping of signals was observed between the TBIS ultrasonics and KardiaMobile 19-kHz signals (Fig. 5a). However, this result was not

observed for the 30-second test performed using the KardiaMobile app. Nevertheless, when different individuals operated the TBIS and KardiaMobile app, ECG results could be obtained without any interference. When a single investigator operated the TBIS, however, even in the absence of ultrasounds, the KardiaMobile did not provide accurate ECG readings. This finding indicates that the Kardia algorithm may be designed to analyze resting heartbeats and ECG recordings only under normal breathing conditions (Fig. 5b).

Correlation between audio ultrasonic signals and visual observations

A high degree of correlation was observed between the duration measurements obtained using audio or video, with R^2 values ranging from 0.9993 to 0.9999 being obtained (N = 39–48). These findings may be useful for developing software and algorithms for determining the duration of specific ultrasonic frequencies, such as 18 kHz (pink ball), 20 kHz (yellow ball), and 22 kHz (green ball; Fig. 6 and Table 3).

Discussion

In this study, we demonstrated that coupling IR detection of ball movement and the transmission of ultrasonic signals at 18–22 kHz using our designed attachment for TBISs can be feasibly used to wirelessly transmit real-time TBIS data. In addition, we determined that the recorded ball movements were highly correlated with our direct visual observations of the TBIS. These findings indicate that our design can be used to improve traditional TBISs by equipping them with digital and wireless capabilities.

Our findings were obtained in a laboratory environment, where we tested for both background and artificial noises. We determined that these noises did not affect the accuracy of the ultrasonic signal transmission facilitated by our design. Traditionally, assessment of TBIS performance has been based on Fisher's formula[7] or the maximal breathing capacity score.[11] Respiratory strength can be more easily determined using a TBIS than using other

methods, such as chest wall movement analysis.[12] Our proposed design has potential to meet the clinical demand for electronic incentive spirometers.[13,14] Our design does not impair the physical structure or function of TBISs, and the attachment can be easily detached and replaced.

Incorporating this proposed wireless design may improve patient care. Although numerous conflicting results have been obtained regarding the clinical effectiveness of TBISs, the practices and routines associated with the TBIS are often biased. Moreover, patient compliance and adherence in studies involving TBISs are low. In addition, the severity of diseases and surgical procedures vary. Evidence regarding TBISs is insufficient for a conclusive judgment to be made on its effectiveness.[15] A digitized and wirelessly connected TBIS may be beneficial for health-care professionals and researchers. They can use such a device to assess patient outcomes after interventions. Furthermore, such a device can be used to distinguish subgroups on the basis of their compliance and regimens, allowing for a more precise statistical comparison of such groups.[16–18]

According to the precedent set by the AliveCor Heart Monitor, which received Food and Drug Administration 510K approval (K140933) on December 3, 2014,[10] ultrasonic wireless applications of TBISs and other medical devices connected with smartphones can expedite the regulatory process. In the present study, our integration of ultrasonic technology with an IR sensor for use on a TBIS device can be used to determine the duration of the period in which TBIS balls remain afloat, providing on/off signals as performance indicators. Our design can facilitate the digitalization of performance metrics on smartphones and can facilitate the use of TBIS devices in clinical settings, home-based rehabilitation monitoring, and telehealth services. Health-care professionals can use our design to monitor TBIS compliance, patient goals, and achievements without being required to use Bluetooth pairing or WiFi AP password entry. Advanced medical examinations, such as respiratory sinus

arrhythmia analysis, are used to analyze the relationship between ECG and deep breathing.[19] When used in conjunction with portable ECG devices, such as smartwatches, AliveCor, and 24-hour continuous ECG monitors, our ultrasonic TBIS design can provide valuable reference data, offering insights into inspiration patterns when ECG recordings are analyzed.

Although the broad-line sensitivity is lower for lower frequency ranges in iOS devices, the algorithm can still distinguish ultrasounds and confirm the status of TBIS balls. Given that sound travels at approximately 340 m/s, no substantial concerns related to accuracy and latency exist when a smartphone is used as a real-time display for TBIS performance. Moreover, in our design, the ultrasonic intensity can be adjusted and set to default frequencies, such as 18.5, 19, 19.5, 20.5, 21, and 21.5 kHz, which can prevent cross-interference and improve sensitivity when multiple users are involved. A spectrogram of a 10-to-30-s recording can be analyzed to establish or calibrate the optimal threshold for distinguishing background noise from ultrasonic signals. Therefore, our design facilitates dynamic sensitivity adjustment of ultrasonic wireless technology, which widens its applicability across diverse scenarios.

This study has several limitations that should be addressed. First, the device attachment we developed is a prototype of the design. Thus, its durability is yet to be thoroughly tested. Furthermore, whether it can be easily mounted onto traditional TBISs by everyday users and patients requires further investigation. Second, we tested this design in an ideal environment, and airflow was not provided by a patient. Therefore, the actual efficacy of the device in detecting ball movements and transmitting ultrasonic signals across a diverse patient population in clinical settings remains to be validated. Third, our proposed design can only be coupled with an incentive spirometer with a three-ball design. Other types of incentive spirometers may require different methods for detecting airflow generated by patients. Fourth, we tested only a limited number of noises that were provided by the

investigators, such as music and breathing efforts. To determine the ability of the device to effectively filter various noises users might encounter in their daily activities, further tests involving a broader range of background noises are warranted.

Conclusion

This proposed design, in which an IR sensor is combined with an ultrasonic module transmitting signals ranging from 18 to 22 kHz, can provide excellent wireless signals when a TBIS and Android or iOS smartphones are separated by a distance of 10–160 cm. The design offers an excellent signal-to-noise ratio that may enable the digitalization and wireless transformation of traditional, nonelectronic TBISs. This design can upgrade the functionality of TBISs and enable clinicians, patients, and healthy individuals to understand and monitor respiratory function.

Acknowledgment

The authors thank Genius Holding for providing the ultrasonic wireless modules, audio analysis support, and incentive spirometers.

Conflicts of Interest Declaration

No financial support was received from any other sponsor.

References

1 FDA, U. S. *General Wellness: Policy for Low Risk Devices* (U.S. Food and Drug Administration, 2019).

2 FDA, U. S. *Enforcement Policy for Non-Invasive Remote Monitoring Devices Used to Support Patient Monitoring During the Coronavirus Disease 2019* (U.S. Food and Drug Administration, 2020).

3 FDA, U. S. *Coronavirus Disease 2019 (COVID-19) Emergency Use Authorizations for Medical Devices* (U.S. Food and Drug Administration, 2022).

4 Liao, C. A. *et al.* The Feasibility and Efficiency of Remote Spirometry System on the Pulmonary Function for Multiple Ribs Fracture Patients. *J Pers Med* **11**, doi:10.3390/jpm11111067 (2021).

5 Soh, J. Y. *et al.* A Mobile Phone-Based Self-Monitoring Tool for Perioperative Gastric Cancer Patients With Incentive Spirometer: Randomized Controlled Trial. *JMIR Mhealth Uhealth* **7**, e12204, doi:10.2196/12204 (2019).

6 Kumar, A. S. *et al.* Comparison of Flow and Volume Incentive Spirometry on Pulmonary Function and Exercise Tolerance in Open Abdominal Surgery: A Randomized Clinical Trial. *J Clin Diagn Res* **10**, KC01-06, doi:10.7860/JCDR/2016/16164.7064 (2016).

7 Robert M. Kacmarek, J. K. S., and Albert J. Heuer. *Egan's Fundamentals of Respiratory Care, 12th Edition*. (Elsevier, 2021).

8 Reyes, B. A. *et al.* Employing an Incentive Spirometer to Calibrate Tidal Volumes Estimated from a Smartphone Camera. *Sensors (Basel)* **16**, doi:10.3390/s16030397 (2016).

9 Technologies, T. M. (Tidal Medical Technologies, 2021).

10 AliveCor. (AliveCor, 2012).

11 Loh, L. C. *et al.* Disability and breathlessness in asthmatic patients--a scoring method by repetitive inspiratory effort. *J Asthma* **42**, 853-858, doi:10.1080/02770900500371138 (2005).

12 Chang, A. T., Palmer, K. R., McNaught, J. & Thomas, P. J. Inspiratory flow rate, not type of incentive spirometry device, influences chest wall motion in healthy individuals. *Physiother Theory Pract* **26**, 385-392, doi:10.3109/09593980903423210 (2010).

13 Eltorai, A. E. M. *et al.* Effect of an Incentive Spirometer Patient Reminder After Coronary Artery Bypass Grafting: A Randomized Clinical Trial. *JAMA Surg* **154**, 579-588, doi:10.1001/jamasurg.2019.0520 (2019).

14 Eltorai, A. E. M. *et al.* Financial Impact of Incentive Spirometry. *Inquiry* **55**, 46958018794993, doi:10.1177/0046958018794993 (2018).

15 Eltorai, A. E. M. *et al.* Clinical Effectiveness of Incentive Spirometry for the Prevention of Postoperative Pulmonary Complications. *Respir Care* **63**, 347-352, doi:10.4187/respcare.05679 (2018).

16 Baxter, C., Carroll, J. A., Keogh, B. & Vandelanotte, C. Seeking Inspiration: Examining the Validity and Reliability of a New Smartphone Respiratory Therapy Exergame App. *Sensors (Basel)* **21**, doi:10.3390/s21196472 (2021).

17 Toor, H. *et al.* Efficacy of Incentive Spirometer in Increasing Maximum Inspiratory Volume in an Out-Patient Setting. *Cureus* **13**, e18483, doi:10.7759/cureus.18483 (2021).

18 Ubolsakka-Jones C PhD, P. T., Tasangkar W Msc, P. T. & Jones, D. A. P. Comparison of breathing patterns, pressure, volume, and flow characteristics of three breathing techniques to encourage lung inflation in healthy older people. *Physiother Theory Pract* **35**, 1283-1291, doi:10.1080/09593985.2018.1477890 (2019).

19 Kurisu, S. *et al.* Effects of deep inspiration on QRS axis, T-wave axis and frontal QRS-T angle in the routine electrocardiogram. *Heart Vessels* **34**, 1519-1523, doi:10.1007/s00380-019-01380-7 (2019).

Table 1. Distance and signal levels at different frequencies in Android and iOS smartphones in .wav format

Audition audio intensity (dBFS)	Frequency	Background	10 cm	20 cm	40 cm	80 cm	160 cm
iOS smartphone	18 kHz	−101.34	−18.13	−21.8	−27.99	−33.42	−40.26
	20 kHz	−97.79	−21.23	−25.23	−28.42	−35.51	−43.06
	22 kHz	−118.2	−49.91	−55.62	−57.53	−64.36	−70.14
	Arduino ultrasound 23 kHz	−82.26	−93.41	−101.58	−98.19	−110.92	−82.26
	KardiaMobile 19 kHz	−98.82	−35.17	−35.87	−41.45	−44.93	−59.04
Android smartphone	18 kHz	−115.68	−33.35	−35.86	−41.88	−47.67	−77.66
	20 kHz	−107.64	−35.96	−41.08	−44.25	−50.55	−84.86
	22 kHz	−108.14	−38.57	−45.38	−49.19	−54.91	−90.22
	Arduino ultrasound 23 kHz	−111.6	−70.9	−76.41	−94.34	−95.75	−98.33
	KardiaMobile 19 kHz	−108.54	−54.19	−56.8	−65.25	−79.94	−77.74
External MIC + iOS smartphone	18 kHz	−96.51	−13.99	−13.66	−20.61	−28.14	−32.77
	20 kHz	−103.13	−20.41	−19.01	−24.68	−29.81	−36.3
	22 kHz	−109.49	−22.6	−22.58	−24.07	−29.8	−36.61
	Arduino ultrasound 23 kHz	−104.68	−82.46	−94.97	−92.63	−103.18	−102.39
	KardiaMobile 19 kHz	−93.54	−32.07	−32.92	−43.08	−49.94	−58.75
External MIC + Android smartphone	18 kHz	−100.55	−13.07	−13.05	−19.82	−27.05	−32.04
	20 kHz	−71.04	−22.23	−20.02	−23.62	−28.9	−35.24
	22 kHz	−81.68	−22.41	−22.95	−24.83	−30.34	−36.63
	Arduino ultrasound 23 kHz	−80.64	−42.53	−47.8	−50.87	−57.5	−60.92
	KardiaMobile 19 kHz	−94.22	−22.7	−28.62	−30.31	−38.59	−54.76

Table 2. Signal and noise levels at differential frequencies at a distance of 50 cm in Android and iOS smartphones in .wav format

Audition audio intensity (dBFS)	Frequency (kHz)	Office and Laboratory		YouTube Music	
		Noise	Signal + Noise	Noise	Signal + Noise
iOS smartphone	18	−101.34	−47.01	−102.53	−47.64
	20	−97.79	−45.66	−100.09	−47.16
	22	−118.2	−89.05	−118.71	−76.13
iOS smartphone + USB-MIC	18	−96.51	−51.85	−88.26	−42.13
	20	−103.13	−48.32	−86.57	−45.04
	22	−109.49	−45.72	−96.07	−44.03
Android smartphone	18	−115.68	−66.36	−93.94	−65.12
	20	−107.64	−65.61	−91.04	−62.73
	22	−108.14	−86.72	−111.01	−61.64
Android smartphone + USB-MIC	18	−100.55	−37.34	−83.92	−39.95
	20	−71.04	−38.22	−77.71	−44.36
	22	−81.68	−37.94	−83.98	−35.52

Table 3. Duration and deviation of visual observations and ultrasonic recordings of each floating ball

Ball 1			Ball 2			Ball 3		
Ultrasound (s)	Video (s)	Deviation	Ultrasound (s)	Video (s)	Deviation	Ultrasound (s)	Video (s)	Deviation
3.17	3.13	1.3%	2.29	2.23	2.7%	-	-	-
4.04	4.00	1.0%	3.26	3.23	0.9%	3.15	3.14	0.3%
1.13	1.09	3.6%	1.07	1.03	3.8%	0.29	0.26	10.9%
1.08	1.01	6.7%	-	-	-	-	-	-
1.20	1.14	5.1%	0.27	0.25	7.7%	-	-	-
2.08	2.01	3.4%	1.27	1.25	1.6%	-	-	-
5.08	5.06	0.4%	5.01	5.00	0.2%	4.19	4.18	0.2%
4.09	4.05	1.0%	4.02	4.00	0.5%	3.12	3.09	1.0%
3.28	3.24	1.2%	-	-	-	-	-	-
2.14	2.10	1.9%	1.2	1.17	2.5%	-	-	-
4.19	4.16	0.7%	4.12	4.09	0.7%	4.01	4.00	0.2%
4.14	4.12	0.5%	4.07	4.04	0.7%	3.23	3.19	1.2%
3.23	3.18	1.6%	3.08	3.04	1.3%	-	-	-
5.03	5.00	0.6%	4.25	4.23	0.5%	4.12	4.08	1.0%
2.29	2.29	0.0%	2.19	2.18	0.5%	0.26	0.23	12.2%
2.26	2.21	2.2%	2.12	2.09	1.4%	0.29	0.27	7.1%
2.18	2.16	0.9%	2.09	2.06	1.4%	0.29	0.27	7.1%
1.15	1.14	0.9%	1.09	1.07	1.9%	0.28	0.26	7.4%
2.09	2.06	1.4%	2.02	2.00	1.0%	1.10	1.09	0.9%
2.21	2.19	0.9%	2.15	2.12	1.4%	1.20	1.17	2.5%
2.03	2.02	0.5%	1.27	1.25	1.6%	1.17	1.16	0.9%
2.26	2.25	0.4%	2.17	2.14	1.4%	2.00	2.00	0.0%
2.18	2.16	0.9%	2.12	2.09	1.4%	1.16	1.12	3.5%
2.11	2.09	1.0%	2.02	1.99	1.5%	1.07	1.15	7.2%
3.03	3.02	0.3%	2.27	2.25	0.9%	2.17	2.16	0.5%
4.19	4.17	0.5%	4.13	4.12	0.2%	4.03	4.02	0.2%
1.01	1.00	1.0%	0.26	0.23	12.2%	0.16	0.15	6.5%
1.27	1.25	1.6%	1.21	1.18	2.5%	1.09	1.06	2.8%
2.06	2.03	1.5%	1.28	1.26	1.6%	1.18	1.17	0.9%
4.02	4.00	0.5%	3.25	3.23	0.6%	3.11	3.10	0.3%
3.11	3.09	0.6%	3.02	3.01	0.3%	-	-	-
4.09	4.07	0.5%	4.05	4.03	0.5%	3.26	3.25	0.3%
3.24	3.23	0.3%	3.16	3.16	0.0%	3.01	3.00	0.3%
1.18	1.16	1.7%	1.08	1.07	0.9%	0.27	0.26	3.8%
4.04	4.03	0.2%	3.29	3.27	0.6%	3.19	3.17	0.6%
4.07	4.06	0.2%	4.02	4.01	0.2%	3.21	3.20	0.3%
2.09	2.06	1.4%	1.09	1.28	16.0%	-	-	-
2.09	2.08	0.5%	2.02	2.00	1.0%	1.23	1.19	3.3%
1.27	1.25	1.6%	1.21	1.18	2.5%	1.06	1.04	1.9%
2.12	2.09	1.4%	2.03	2.00	1.5%	1.10	1.08	1.8%
3.25	3.24	0.3%	3.18	3.16	0.6%	2.29	2.27	0.9%
3.27	3.26	0.3%	3.21	3.18	0.9%	3.10	3.09	0.3%
4.06	4.05	0.2%	3.29	3.28	0.3%	3.16	3.14	0.6%
3.03	3.02	0.3%	2.25	2.23	0.9%	2.13	2.12	0.5%
3.11	3.09	0.6%	3.04	3.01	1.0%	2.11	2.10	0.5%
2.09	2.07	1.0%	1.29	1.28	0.8%	1.04	1.01	2.9%
2.29	2.26	1.3%	2.21	2.21	0.0%	2.10	2.08	1.0%
3.24	3.22	0.6%	3.17	3.16	0.3%	3.06	3.06	0.0%

Figure Captions

Fig. 1. Three-ball incentive spirometer with ultrasonic wireless modules and test photos.

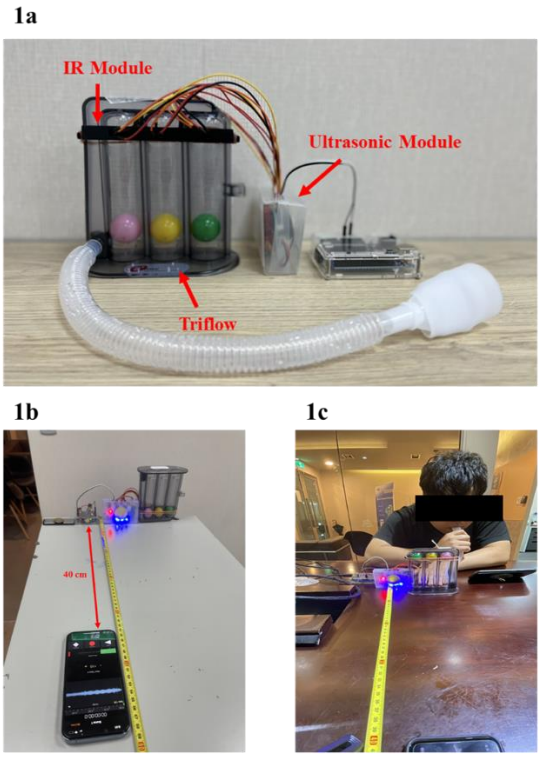

Fig. 2. Spectrograms of ultrasonics in iOS and Android smartphones without or with an external MIC with different distances between the ultrasonic module and smartphone microphone.

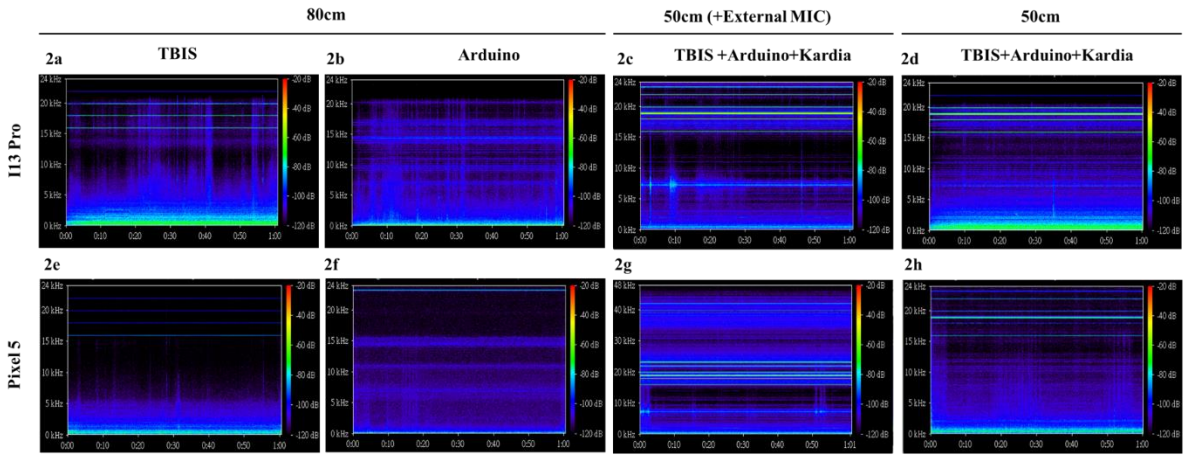

Fig. 3. Noise interference and ultrasonic signals in the spectrogram with a noise speaker distance of 40 cm separating the ultrasonic module and smartphone microphone.

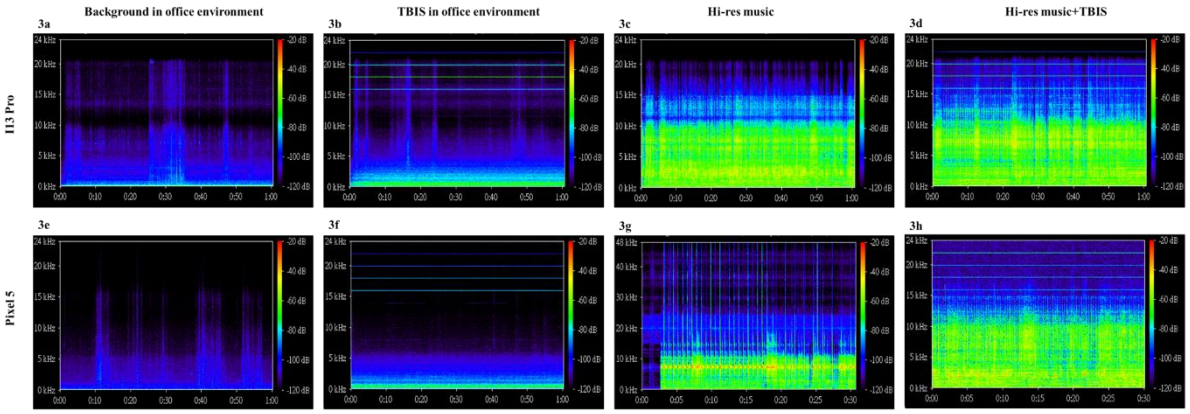

435

436 Fig. 4. Spectrogram of the IR plus ultrasonic signal at reverse status, 3-L syringe suction, and

437 human inspiration breath with a distance of 40 cm separating the ultrasonic module and

438 smartphone microphone.

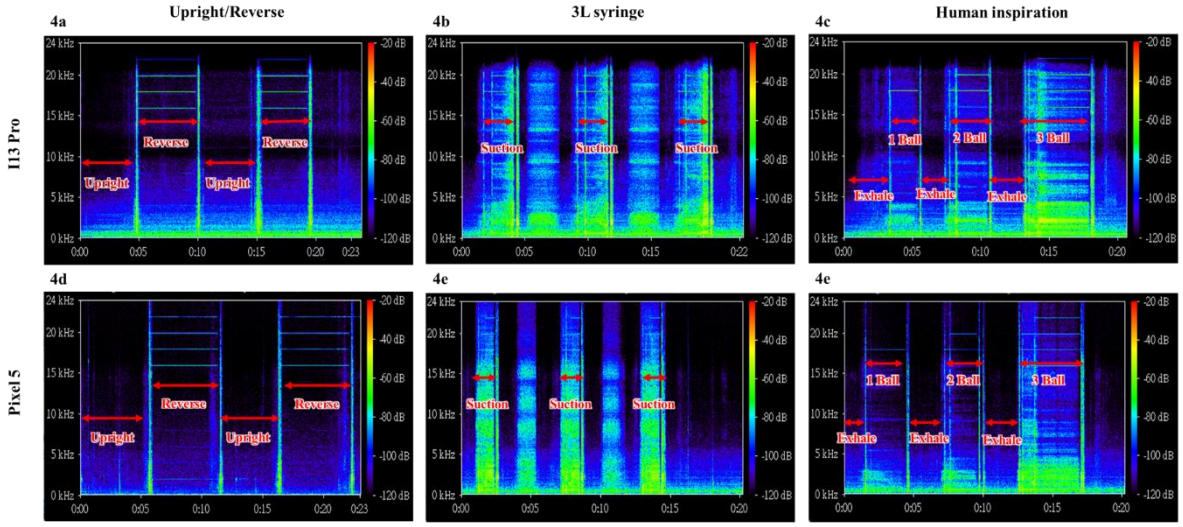

439

440 Fig. 5. Comprehensive results of incentive spirometry and single-lead ECG.

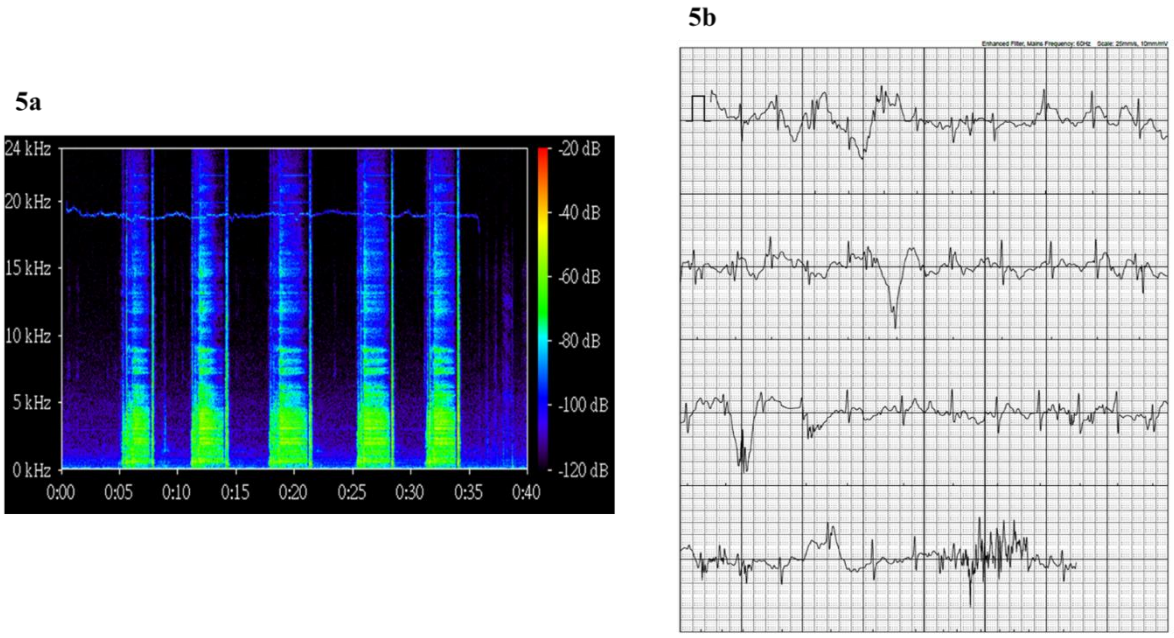

441

442 Fig. 6. Correlation of visual observations and ultrasonic recordings of the duration of each

443 ball floating on the top.

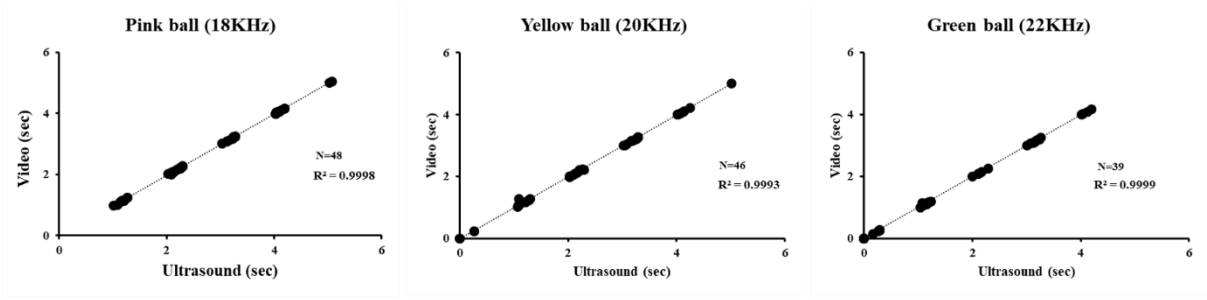

444